Award number: 03HQGR0100

REFINING THE SOUTHERN CALIFORNIA 3D MODEL IN THE LOS ANGELES AREA

Lupei Zhu
Saint Louis University
Department of Earth and Atmospheric Sciences, SLU, St Louis, MO 63103
email: lupei@eas.slu.edu; Tel: 314 977-3118; Fax: 314 977-3118

Program Element: II
Key Words: wave propagation, seismotectonics, strong ground motion

Research supported by the U.S. Geological Survey (USGS), Department of the Interior, under USGS award number 03HQGR0100. The views and conclusions contained in this document are those of the authors and should not be interpreted as necessarily representing the official policies, either expressed or implied, of the U.S. Government.

Award number: 03HQGR0100

REFINING THE SOUTHERN CALIFORNIA 3D MODEL IN THE LOS ANGELES AREA

Lupei Zhu
Saint Louis University
Department of Earth and Atmospheric Sciences, SLU, St Louis, MO 63103
email: lupei@eas.slu.edu; Tel: 314 977-3118; Fax: 314 977-3118

Abstract

A three-dimensional velocity model of the Los Angeles Basin has been developed by the Southern California Earthquake Center (SCEC) for simulating strong ground motion, analyzing site effects, and locating earthquakes. P-wave velocities in this model are derived from oil logs, stratigraphic surfaces, and seismic tomography. S-wave velocities and densities are determined by empirical rules. To verify and refine the SCEC model, we obtained 509 teleseismic receiver functions at five broadband stations in the Los Angeles Basin. Receiver functions of all five stations show strong azimuthal variations that are related to basin geometry. The SCEC-3D model is inadequate in predicting the observed receiver function waveforms. We modeled those variations using the generalized ray theory and finite difference (FD) methods and obtained basin thicknesses, P and S velocity contrasts, and the geometry of the basement interface beneath the five stations.

Non-Technical Abstract

We processed 22,144 three-component waveforms from 663 global large earthquakes between 2000 and 2003 and obtained 9,199 high quality receiver functions of 35 broadband stations in the Los Angeles area. We identified 20 stations whose receiver functions show characteristics of sedimentary basin effects. Their locations correlate well with distribution of sedimentary basins in the Los Angeles areas from geology. Modeling of receiver functions of five basin stations shows that sedimentary basins have high V_p/V_s ratio of 2.3 to 2.5. The SCEC-3D model over-estimates the sedimentary basin thickness near station USC. We obtained basin thicknesses, P and S velocity contrasts, and the geometry of the basement interface beneath the five stations.

1 Introduction

The Los Angeles Basin is located beneath the metropolitan Los Angeles (Figure 1). The area has previously undergone a complex multiphase structural process including subductions in the Cretaceous and early Paleogene, Paleogene terrane accretion, and mid-Miocene rifting and block rotation. The basin was formed in the late Neogene on a continental margin as a result of regional crustal extension [*Wright*, 1991; *Biddle*, 1991]. During last 20 Ma, about 10 km of marine and alluvial sediments were deposited at the center of the basin. The basin is now surrounded by the Transverse Ranges, San Andreas Fault system, Peninsular Ranges, and Continental Borderland of Southern California (Figure 1). Because of the dense population and developed industries, the Los Angeles Basin is a place with great earthquake hazard.

Regional seismic velocity models are used for earthquake relocation [*Shaw and Shearer*, 1999, e.g.], strong ground motions estimation [*Olsen*, 2000; *Komatitsch et al.*, 2004, e.g.], and site effect analysis [*Vidale and Helmberger*, 1988, e.g.]. In 2000, SCEC released a 3D velocity model (Version 2.0) [*Magistrale et al.*, 2000]. In the Los Angeles area, the model consists of three stratigraphic surfaces: the base of Repetto, the base of Mohnian, and the top of the basement [*Wright*, 1991]. The P-wave velocity in the model is determined by the maximum burial depth and age of the sediment. The S-velocity and density are calculated from the P velocity by empirical rules. Outside the basin, V_p and V_p/V_s ratio are constructed from seismic tomographic results [*Hauksson*, 2000].

Since the velocities and densities are obtained indirectly, there are large uncertainties. These uncertainties prevent us from using the basin model effectively. *Olsen* [2000] used the SCEC 3D model to compute synthetic seismograms of the 1994 Northridge earthquakes with the finite difference method. The result shows that the amplitudes and durations between data and synthetics agree within a factor of two. But the fits among different phases vary considerably. By computing the first- and second-order derivatives of the velocity field of the SCEC-3D model in the vertical direction, *Suss and Shaw* [2003] pointed out the abrupt changes in velocity gradients at the stratigraphic surfaces inside the basin. They also found that the velocities at the basin borders were overestimated, while the velocities at the basin center were underestimated.

In this study, we will refine the 3D structure and velocity contrast of the Los Angeles Basin using teleseismic receiver function data and the finite-difference waveform modeling method.

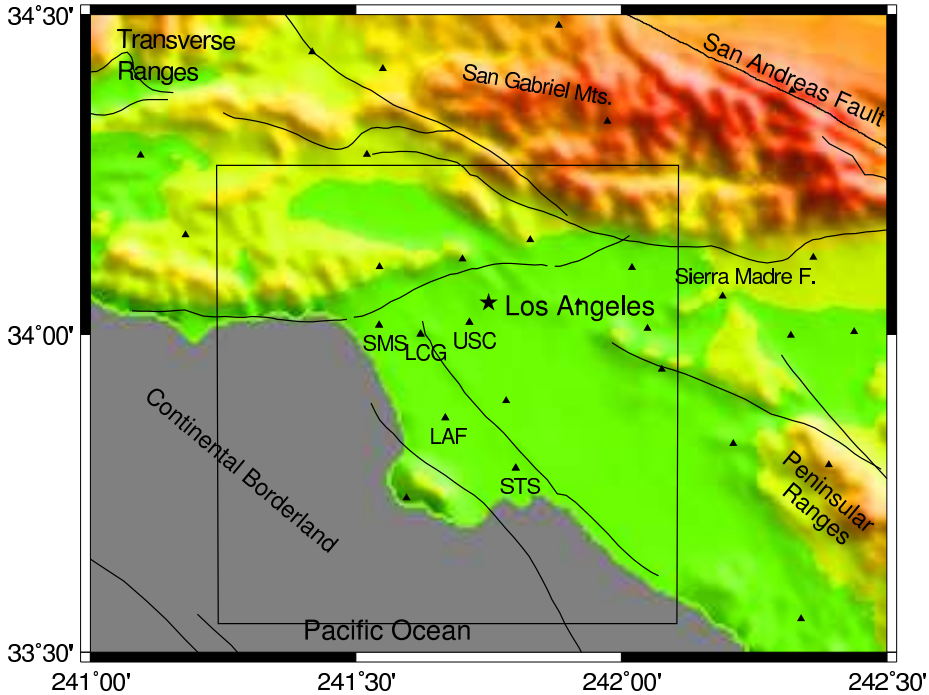

Figure 1: Topographic map of the Los Angeles area. The box is the study area. Thin lines are faults and triangles denote broadband seismic stations. The five basin stations used in this study are labeled by their names.

2 Data and Results

2.1 Receiver functions of stations in the Los Angeles Area

We retrieved waveform recordings of all earthquakes with magnitude larger than 5 between 2000 and 2003 from the Data Center of Southern California Earthquake Center. 35 broadband stations in the Los Angeles Area were used (Fig. 1). After a quick visual inspection of all the waveforms, 22,144 three-component waveforms from 663 events were selected based on their good signal-to-noise ratios. From the event distribution shown in Fig. 2, one can see that we have good azimuthal coverage, especially for the west and northwest directions. It served as a data quality check to identify instrument problems such as polarity reversal. We then used an iterative time-domain deconvolution technique to compute receiver functions [*Kikuchi and Kanamori*, 1982; *Ligorria and Ammon*, 1999]. This deconvolution technique has better performance than other deconvolution methods especially for noisy data. A graphics user interface program were written using TCL/TK language to allow us to visually examine deconvolution traces of each station. This was done by sorting traces by back-azimuth and checking for similarities among receiver functions from clustered events.

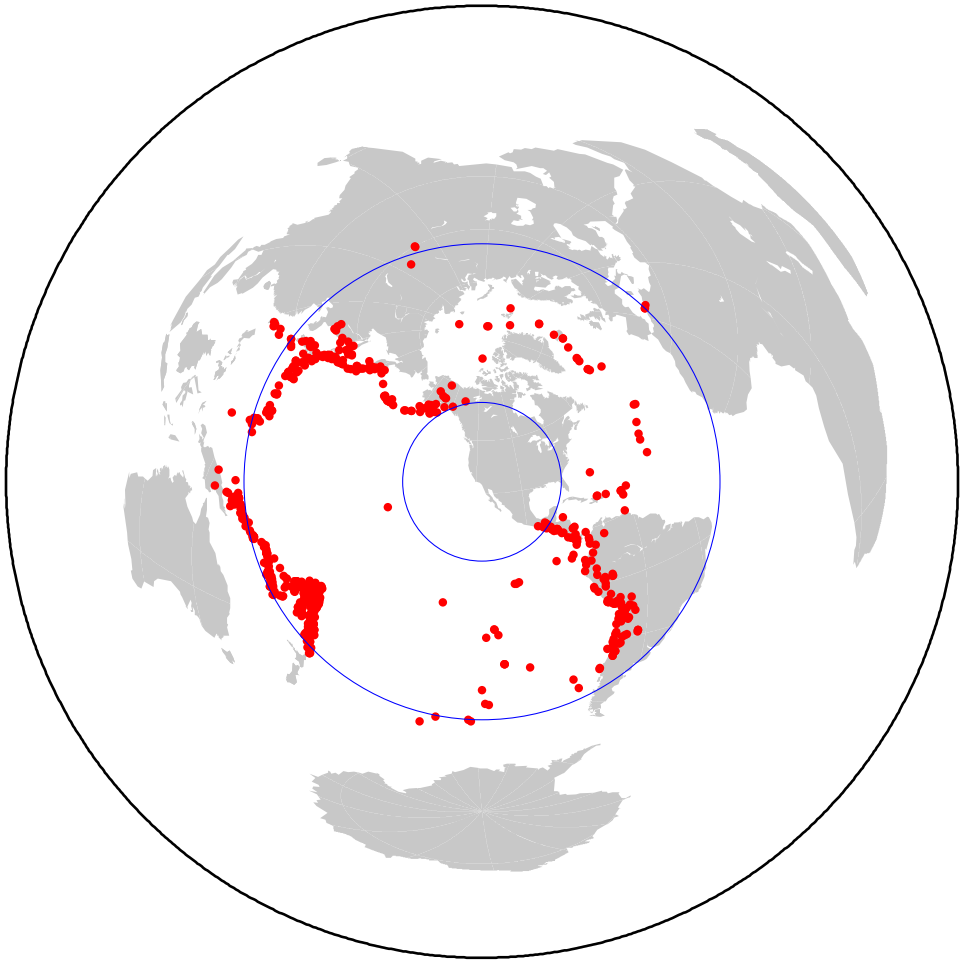

Figure 2: Distribution of 663 teleseismic events between 30° and 90°in epicentral distance.

Bad deconvolution traces were discarded. In total we obtained 9,199 receiver functions, about 260 receiver functions per station on average.

For each station, we stacked receiver functions if they cluster in the coordinates of back-azimuth and ray-parameter. We then plotted back-azimuthal profiles of radial and tangential receiver functions. Fig. 3 shows an example for station USC. This lets us to examine shapes of receiver functions and their variation with directions. The first 10 s of receiver functions following the direction P wave are very diagnostic to existence of sedimentary layer, which tends to reduce the amplitude of the direct P wave and generates large amplitude P-to-S converted waves on the radial component. These converted waves reverberate in the sedimentary layer and dominate the first 10 s of receiver function. Large tangential amplitudes are often observed due to lateral variation of basin thickness.

We have identified 20 stations whose receiver functions show characteristics of basin effects similar to those at station USC (Fig. 3). Their locations are shown in Fig. 1 and correlate well with distribution of sedimentary basins in the Los Angeles areas.

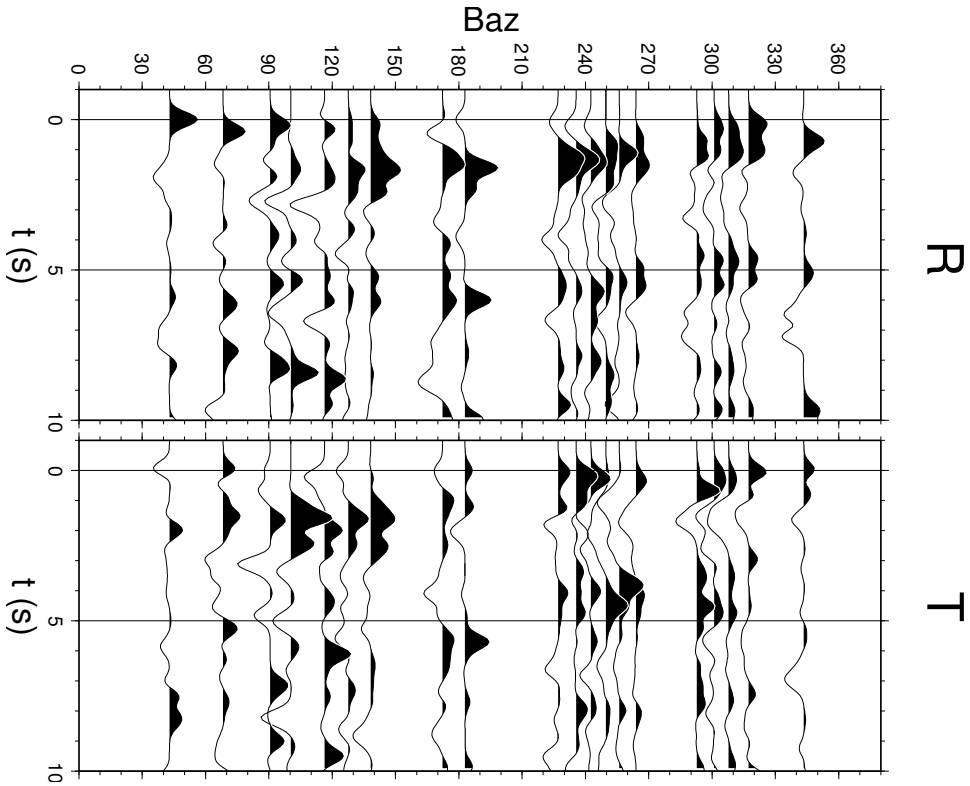

Figure 3: Radial and tangential components of receiver functions of station USC.

2.2 1-D Inversion of receiver functions

We conducted inversions of the first 10 s radial receiver functions for upper crustal velocity structure under each station using the Neighborhood Algorithm (NA) [*Sambridge*, 1999]. It is a multi-dimensional parameter space search algorithm that only needs solving the forward problem and does not require computing partial derivatives of receiver functions. We used a two-layer upper crustal model with the bottom layer (the basement) velocities fixed (V_p 6 km/s and V_s 3.43 km/s). The velocities in the top layer are assume to be linear functions of depth with a constant V_p/V_s ratio. We searched for the best thickness, top and bottom shear velocities, and V_p/V_s ratio of the sedimentary layer that produce the best fit in a least-square sense to observed receiver functions. Theoretical receiver functions are calculated using the Haskell propagator matrix method [*Haskell*, 1964]. Because of good incidence angle sampling for the SE direction (back-azimuths 110° to 140°) and the NW direction (back-azimuth 290° to 330°), we did inversions of receiver functions of these two directions separately. A wide range of parameters (basin depths from 0.5 to 8 km and shear velocities from 0.2 to 3.0 km/s) were searched.

Fig. 4 shows inversion results for station USC and their comparison with the SCEC-3D (version 3) model. For the NW direction, the best model has a basin thickness of 2.3 km and a V_p/V_s ratio of 2.36. The best model from the inversion of SE receiver functions shows

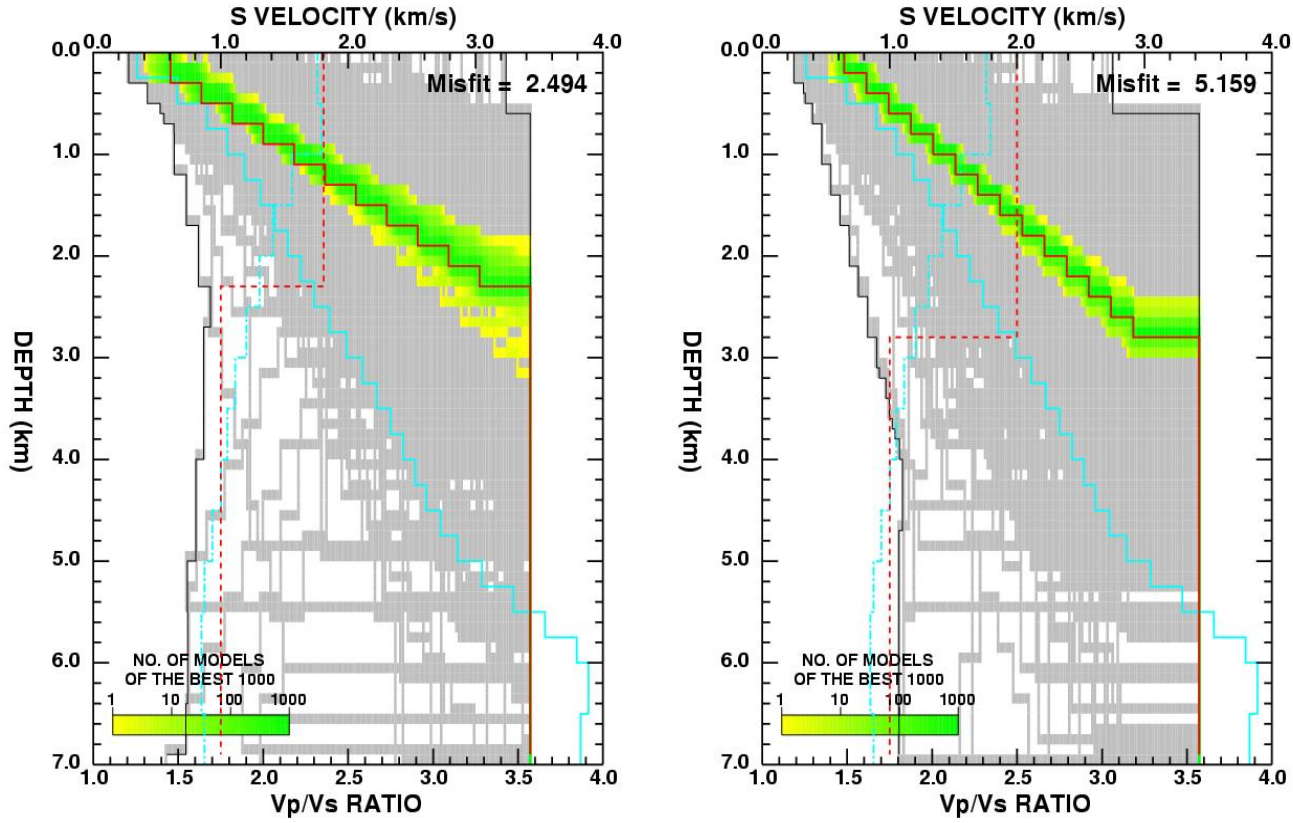

Figure 4: NA inversion results for the NW (left) and SE (right) directions. The Gray area shows all models searched in the NA inversion and the colored area represents the best 1000 models. The red solid line is the best shear velocity model and the red dashed line is the best V_p/V_s model. The corresponding SCEC-3D models are shown in blue color.

a slightly thicker sedimentary layer (2.8 km). The obtained V_p/V_s ratio is close to that of the SCEC-3D model but the basin thickness is much less than that of the SCEC-3D model (6 km). The theoretical receiver functions of the best models match main features of the observed radial receiver functions (Fig. 5).

2.3 3-D modeling of receiver functions

2.3.1 Validation of the SCEC veclocity model

To validate the SCEC-3D velocity model, we generated an 80 km×80 km×80 km cube containing the basin. The velocities are clamped to $V_{p_{min}} = 2.41$ km/s, $V_{s_{min}} = 1.0$ km/s and $V_{p_{max}} = 6.1$ km/s, $V_{s_{max}} = 3.52$ km/s to make sure that the finite-difference (FD) computation is accurate up to 1 Hz. we also removed the artificial boundary in the model while keeping the shape of the basin and velocity contrast the same.

Table 1: Best-fit Basement Interface

Sta	h (km)	Vs contrast	Vp contrast	strike	dip
LAF	3.4	2.16/3.66	3.97/6.00	300	10
LCG	3.4	2.16/3.66	3.97/5.00	285	15
SMS	3.6	2.16/3.66	3.97/6.00	270	25
STS	3.8	2.16/3.66	3.97/6.00	300	10
USC	4.6	2.52/3.49	4.55/5.96	105	20

Figure 7 shows comparison of observed and predicted receiver functions at station STS. The predictions do not match the observed well. The amplitudes of P-to-S converted wave around 1 s are smaller on both radial and tangential components. The relative arrival times of P-to-S converted wave are not consistent with data either. These indicate that the velocity contrast of the basement interface is not large enough and the shape of the basin needs to be modified.

2.3.2 Refining the Los Angeles Basin velocity model

We noticed that receiver functions of all stations in the Los Angeles Basin show systematic variations with azimuth. For example, at station STS (figure 7) the polarization of P-to-S converted wave on the tangential component reverses at about 210°, and the amplitudes of the converted wave increase to both sides. The relative arrival times of converted wave for all azimuths are almost identical. These features indicate that bottom of the basin beneath each station can be modeled as a single dipping interface. To find the best dipping structure for each station, we used a ray-based method [*Langston*, 1977] to compute synthetic receiver functions to model the observed waveforms of the station.

The velocity model is constructed by

$$V_p(h) = a + bh^{\frac{1}{6}} \tag{1}$$

where V_p is P-wave velocity, a and b are two constants for each station. h is the burial depth of sediments. This velocity profile is very close to the SCEC model. The V_s and density are calculated using the same formula as in the SCEC model. The minimum V_s is constraint to 0.5 km/s.

The synthetic receiver functions from the best dipping model agree with the observed receiver functions well in both amplitude and arrival time (Figure 8). For example, at the station STS, the P-wave velocity jumps from 4.0 km/s in the basin to 6.0 km/s in the basement. The strike and dip of the interface is 300° and 10°, respectively (Figure 9). Similar parameters for other stations are listed in Table 1.

3 Publications

1. Chu, R., and L. Zhu, Refining the southern California 3D model in the Los Angeles area using seismic waveforms, *Eos Trans. AGU*, *84 (46)*, Fall Meeting Suppl., Abstract S32A–0843, 2003.

2. Chu, R., and L. Zhu, Improvement of the SCEC-3D model of the Los Angeles Basin using teleseismic receiver functions, *Eos Trans. AGU*, *86*, Fall Meeting Suppl., Abstract S43B–1070, 2005.

4 Data availability

In addition to velocity models listed in Table 1 of the report, a CCP crustal image along the LABSE line in PDF format and station delays in ASCII format are available in ftp.eas.slu.edu-/pub/lupei/labpse.grd.tz. For detailed information, contact Lupei Zhu (email: lupei@eas.slu.edu, Tel: 314 977-3118).

References

Biddle, K. T., The los angeles basin: An overview, *AAPG Mem.*, *52*, 5–24, 1991.

Haskell, N. A., Radiation pattern of surface waves from point sources in a multi-layered medium, *Bull. Seismol. Soc. Am.*, *54*, 377–393, 1964.

Hauksson, E., Crustal structure and seismicity distribution adjacent to the pacific and north america plate boundary in southern california, *J. Geophys. Res.*, *105*, 13,875–13,903, 2000.

Kikuchi, M., and H. Kanamori, Inversion of complex body waves, *Bull. Seismol. Soc. Am.*, *72*, 491, 1982.

Komatitsch, D., Q. Liu, J. Tromp, P. Suss, C. Stidham, and J. H. Shaw, Simulations of ground motion in the los angeles basin based upon the spectral-element method, *Bull. Seismol. Soc. Am.*, *94(1)*, 187–206, 2004.

Langston, C. A., The effect of planar dipping structure on source and receiver responses for constant ray parameter, *Bull. Seismol. Soc. Am.*, *67*, 1029–1050, 1977.

Ligorria, J. P., and C. J. Ammon, Iterative deconvolution and receiver-function estimation, *Bull. Seismol. Soc. Am.*, *89*, 1395–1400, 1999.

Magistrale, H. S., S. Day, R. W. Clayton, and R. W. Graves, The scec southern california reference three-dimensional seismic velocity model version 2, *Bull. Seismol. Soc. Am.*, *90(6B)*, S65–S76, 2000.

Olsen, K. B., Site amplification in the los angeles basin from three-dimensional modeling of ground motion, *Bull. Seismol. Soc. Am.*, *90*, S77–S94, 2000.

Sambridge, M., Geophysical inversion with a neighbourhood algorithm–I. searching a parameter space, *Geophys. J. Int.*, *138*, 479–494, 1999.

Shaw, J. H., and P. M. Shearer, An elusive blind thrust fault beneath metropolitan los angeles, *Science*, *283*, 1516–1518, 1999.

Suss, M. P., and J. H. Shaw, P-wave seismic velocity structure derived from sonic logs and industry reflection data in the los angeles basin, california, *J. Geophys. Res.*, *108 B3 ESE13*, 1–18, 2003.

Vidale, J. E., and D. V. Helmberger, Elastic finite-difference modeling of the 1971 san fernando, california earthquake, *Bull. Seismol. Soc. Am.*, *78*, 122–141, 1988.

Wright, T. L., Structural geology and tectonic evolution of the los angeles basin, california, *AAPG Mem.*, *52*, 35–134, 1991.

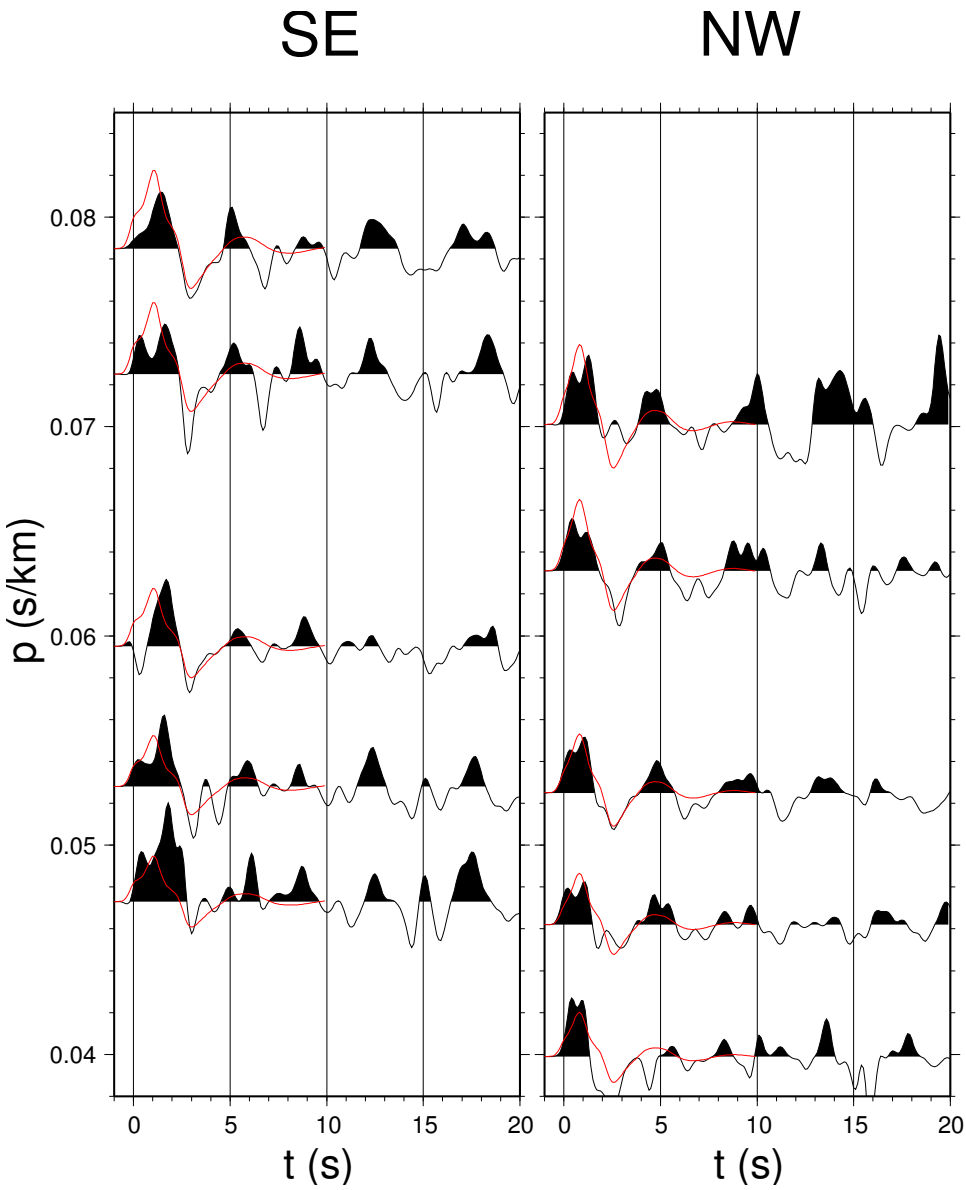

Figure 5: Stacked observed receiver functions from the SE and NW directions. Red colored traces are theoretical receiver functions of the best velocity model from the NA inversions (Fig. 4).

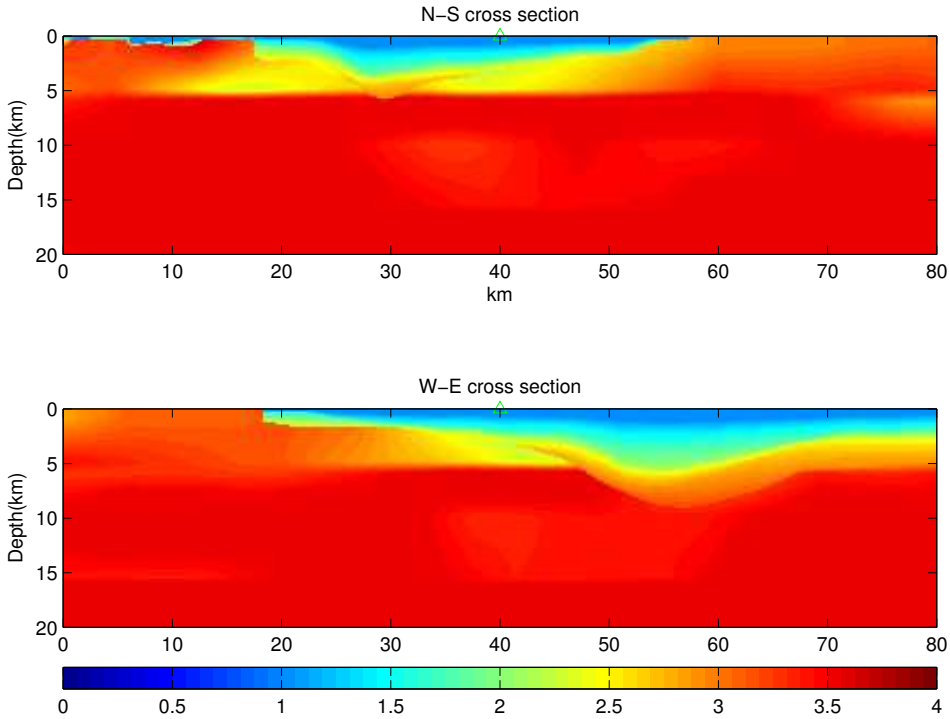

Figure 6: S-wave velocity of the SCEC model in the North-South cross section (upper panel) and West-East cross section (lower panel). See Figure 1 for location of the model. Note the artificial boundary between the model of the sedimentary basin and model of *Hauksson* [2000].

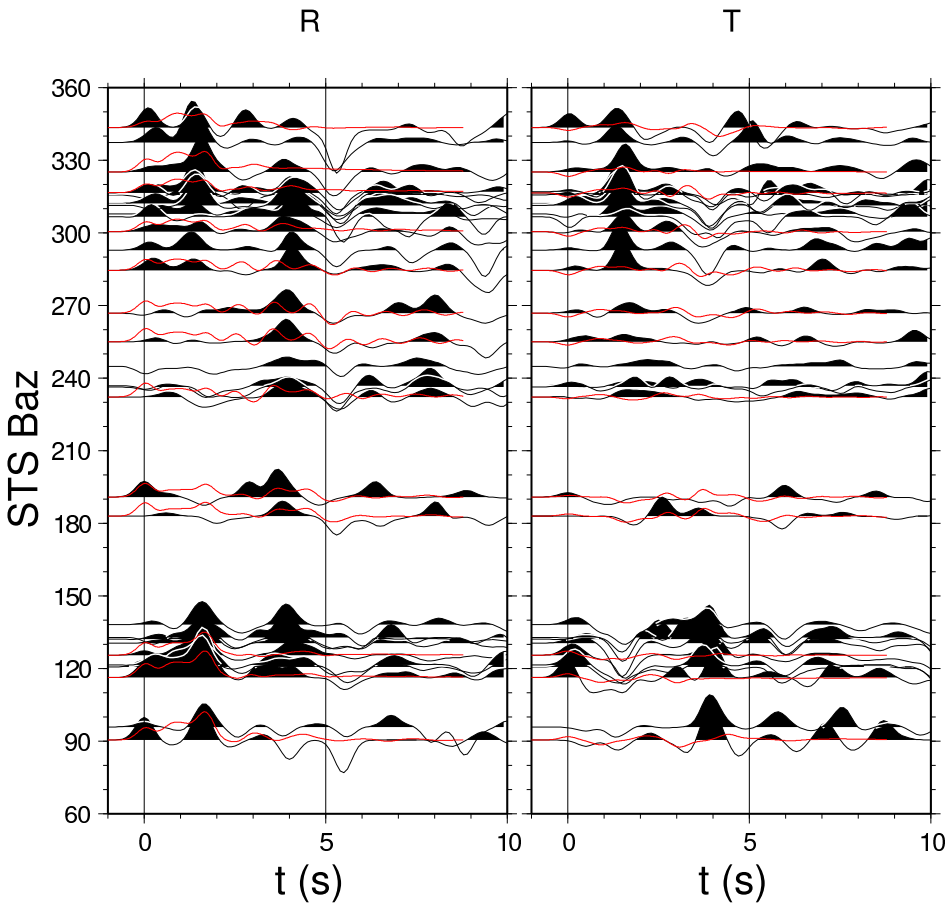

Figure 7: Synthetic and observed receiver functions of station STS.

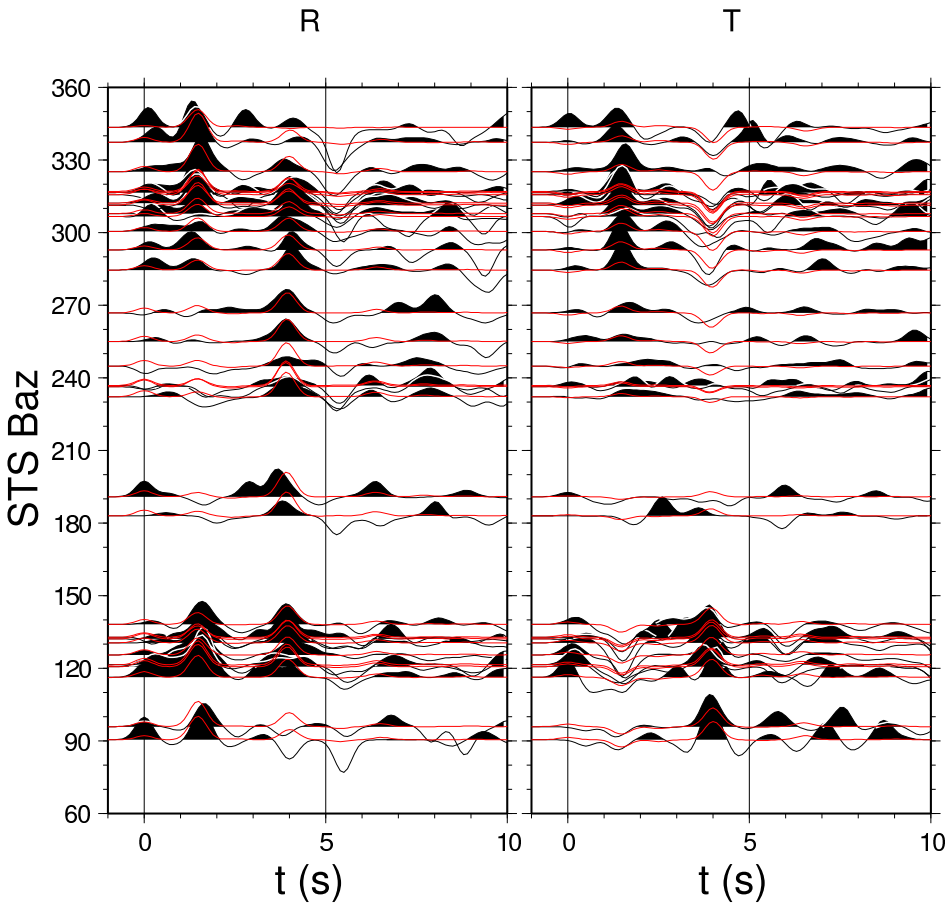

Figure 8: Synthetic and observed receiver functions of station STS. The synthetic receiver functions are calculated by the GRT method.

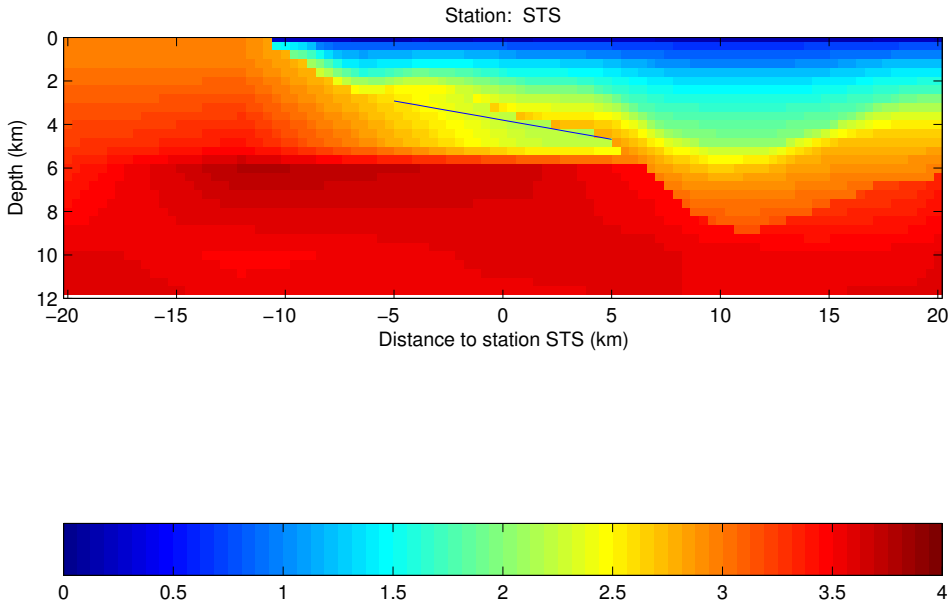

Figure 9: The S-wave velocity cross section perpendicular to the strike direction of the station STS. The blue line is the dipping interface from the GRT method.